

# ComplexBench-Edit: Benchmarking Complex Instruction-Driven Image Editing via Compositional Dependencies

Chenglin Wang<sup>1</sup>, Yucheng Zhou<sup>2</sup>, Qianning Wang<sup>3</sup>, Zhe Wang<sup>1</sup>, Kai Zhang<sup>1</sup>

<sup>1</sup>East China Normal University, China, <sup>2</sup>University of Macau, China,

<sup>3</sup>Auckland University of Technology, New Zealand

52275901013@stu.ecnu.edu.cn, yucheng.zhou@connect.um.edu.mo

## Abstract

Text-driven image editing has achieved remarkable success in following single instructions. However, real-world scenarios often involve complex, multi-step instructions, particularly “chain” instructions where operations are interdependent. Current models struggle with these intricate directives, and existing benchmarks inadequately evaluate such capabilities. Specifically, they often overlook multi-instruction and chain-instruction complexities, and common consistency metrics are flawed. To address this, we introduce **ComplexBench-Edit**, a novel benchmark designed to systematically assess model performance on complex, multi-instruction, and chain-dependent image editing tasks. ComplexBench-Edit also features a new vision consistency evaluation method that accurately assesses non-modified regions by excluding edited areas. Furthermore, we propose a simple yet powerful Chain-of-Thought (CoT)-based approach that significantly enhances the ability of existing models to follow complex instructions. Our extensive experiments demonstrate ComplexBench-Edit’s efficacy in differentiating model capabilities and highlight the superior performance of our CoT-based method in handling complex edits. The data and code are released at <https://github.com/lilly26/ComplexBench-Edit>.

## CCS Concepts

• **Applied computing** → **Multi / mixed media creation**; *Image composition*; • **Computing methodologies** → *Computer vision problems*.

## Keywords

Complex Instruction-Driven Image Editing, Benchmark, Evaluation

## ACM Reference Format:

Chenglin Wang<sup>1</sup>, Yucheng Zhou<sup>2</sup>, Qianning Wang<sup>3</sup>, Zhe Wang<sup>1</sup>, Kai Zhang<sup>1</sup>. 2025. ComplexBench-Edit: Benchmarking Complex Instruction-Driven Image Editing via Compositional Dependencies. In *Proceedings of Make sure to enter the correct conference title from your rights confirmation email (Conference acronym ’ACMMM)*. ACM, New York, NY, USA, 7 pages. <https://doi.org/XXXXXXX.XXXXXXX>

Permission to make digital or hard copies of all or part of this work for personal or classroom use is granted without fee provided that copies are not made or distributed for profit or commercial advantage and that copies bear this notice and the full citation on the first page. Copyrights for components of this work owned by others than the author(s) must be honored. Abstracting with credit is permitted. To copy otherwise, or republish, to post on servers or to redistribute to lists, requires prior specific permission and/or a fee. Request permissions from [permissions@acm.org](mailto:permissions@acm.org).

Conference acronym ’ACMMM, Woodstock, NY

© 2025 Copyright held by the owner/author(s). Publication rights licensed to ACM.

ACM ISBN 978-1-4503-XXXX-X/2018/06

<https://doi.org/XXXXXXX.XXXXXXX>

## 1 Introduction

Text-driven diffusion models have led to remarkable success in image generation and editing [5, 8, 25]. These models have demonstrated impressive capabilities in following single, explicit instructions to modify images, achieving high-fidelity and semantically coherent results [5, 26, 36]. This progress has significantly empowered users to manipulate visual content with natural language.

However, real-world editing often demands more than singular directives. Users frequently issue complex instructions comprising multiple, sometimes interdependent, sub-tasks forming a “chain” where one step’s outcome affects the next (Figure 1). While current models adeptly handle isolated edits, their ability to understand, decompose, and execute such multi-faceted, particularly chain-instruction, inputs is a significant challenge, often leading to incoherent results or failure to meet all constraints.

This limitation stems partly from prevalent evaluation benchmarks. As Table 1 shows, most existing benchmarks primarily test single-constraint or simple independent multi-instruction edits, lacking systematic evaluation for complex, dependent instructions. For example, MagicBrush [36] and I<sup>2</sup>EBench [20], while instruction-driven, overlook multi-instruction and chain-instruction complexities. Complex-Edit [32] addresses multi-instruction editing but not specifically chained dependencies, and its LLM-based consistency evaluation struggles to assess non-modified regions. Furthermore, common L1/L2 consistency metrics are flawed, incorrectly favoring unedited images.

To propel image editing models towards a higher level of intelligence, they must learn “combinatorial reasoning”, the ability to execute instructions correctly under the premise that multiple constraints must hold true simultaneously, especially when these constraints are sequentially dependent. To address the aforementioned limitations and better evaluate the instruction-following capabilities of existing editing models in complex scenarios, this paper introduces **ComplexBench-Edit**, a novel benchmark for image editing specifically designed to assess performance on complex instructions involving multiple combined and dependent modifications. Our benchmark systematically evaluates how well models can handle both parallel and, critically, chain-dependent instructions. Furthermore, we propose a novel vision consistency evaluation method that excludes the influence of modified content by assessing consistency only in the remaining, unaltered regions. We also introduce a simple yet powerful CoT-based approach for image editing. The main contributions of this work are:

- We propose ComplexBench-Edit, a new benchmark tailored for evaluating image editing models on complex, multi-instruction, and chain-dependent instructions, along with a novel vision consistency metric.

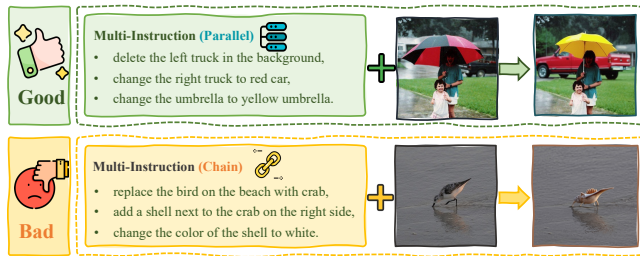


**Figure 1: Comparison between parallel and chain multi-instruction image editing. Parallel editing applies independent instructions simultaneously, while chain editing involves dependent instructions that must be executed in sequence.**

**Table 1: “Ins.,” “Multi-ins.,” “Chain-ins.,” and “Pixel-eval” denote “Instruction-driven,” “Multi-instruction,” “Chain-instruction,” and “Pixel-level image eval”, respectively.**

Datasets / Benchmarks	Ins.	Multi-ins.	Chain-ins.	Pixel-eval
MagicBrush [36]	✓	✗	✗	✓
I <sup>2</sup> EBench [20]	✓	✗	✗	✓
AnyEdit [34]	✓	✗	✗	✓
UltraEdit [38]	✓	✗	✗	✓
PIE-Bench++ [16]	✗	✗	✗	✓
Complex-Edit [32]	✓	✓	✗	✗
Ours (ComplexBench-Edit)	✓	✓	✓	✓

- We provide a detailed analysis of current state-of-the-art image editing models on ComplexBench-Edit, highlighting their strengths and weaknesses in handling complex directives.
- We introduce a simple yet effective CoT-based approach to enhance the complex instruction following capabilities of existing models, demonstrating its effectiveness on our benchmark.

## 2 Related Work

### 2.1 Text-driven Image Editing

Diffusion Models (DMs) [2, 15, 23, 27, 29] have significantly advanced image generation and editing, leading to the Instruction-Based Image Editing (IIE) task where models alter images based on textual instructions. Early IIE milestones include InstructPix2Pix [5], which was trained on synthetic data from GPT-3 [6] and Prompt-to-Prompt [14]. Performance was further improved by works like MagicBrush [36], UltraEdit [38], SEED-Data-Edit [11], HumanEdit [3], and AnyEdit [34], which utilized high-quality curated datasets. More recently, Large Language Models (LLMs) [39, 40] have been integrated to enhance instruction comprehension. For instance, MGIE [10] and SmartEdit [17] leverage Multimodal Large Language Models (MLLMs) for precise guidance. OmniGen [31] employs Phi-3 [1] to strengthen instruction understanding, while Step1X-Edit [19] uses MLLMs [4] for accurate parsing and fine-tunes on quality datasets. ICEdit [37] adopts DiT-based models [22] for their strong generative power. Despite excellent performance on single-instruction tasks, the ability of these models to process and understand complex multi-instruction or chained instructions remains largely unevaluated.

### 2.2 Image Editing Benchmarks

Various benchmarks have recently emerged to advance image editing. MagicBrush [36], based on COCO [18], evaluates instruction

following and consistency using metrics like CLIP [24], DINO [35], L1, and L2 distances. I<sup>2</sup>EBench [20] expanded editing types with 16 evaluation dimensions for comprehensive assessment. Prompt-based benchmarks like PIE-Bench++ [16], OIR-Bench [33], and LOMOE-Bench [7] evaluate multi-object editing but differ from instruction-based methods by requiring image-caption pairs. While these benchmarks have driven progress, they mainly focus on single-instruction editing or specific descriptive inputs. Complex-Edit [32] addresses complex instructions by integrating atomic tasks via a “Chain-of-Edit” pipeline, but it overlooks the specific challenges of chain-instruction scenarios. Therefore, a systematic benchmark for detailed evaluation in complex, particularly chained, scenarios is crucial.

## 3 ComplexBench-Edit

We will detail the construction of our ComplexBench-Edit dataset. The overall data creation pipeline is shown in Figure 2.

### 3.1 Dataset Construction

**3.1.1 Vision Content Filter.** The Vision Content Filter represents the initial and essential stage in our dataset construction pipeline. Its primary objective is to select source images that are suitable for generating complex editing instructions, based on an analysis of their visual content. A fundamental requirement for defining object-centric editing tasks is understanding the objects present in an image. This requires applying an object detection model to identify and localize objects. However, since our source dataset, MSCOCO [18], provides rich ground-truth annotations, we leverage these directly, bypassing the need for a separate detection process. Specifically, we use the annotated bounding boxes, which accurately indicate both the class and location of each object within an image  $I$ . We introduce two filtering criteria:

**1. Intra-class Frequency Constraint.** To reduce ambiguity when referring to multiple instances of the same object category in textual instructions, we restrict the number of objects per class. Let  $N_c(I)$  denote the number of instances (i.e., bounding boxes) of class  $c$  in image  $I$ . We discard image  $I$  if there exists any class  $c$  such that:

$$\exists c \in C(I), \quad N_c(I) > 2 \quad (1)$$

This ensures that no object category appears more than twice in any selected image, simplifying unambiguous reference.

**2. Category Diversity Constraint.** To ensure visual complexity and semantic richness—key for generating multi-object editing instructions—we require a minimum level of object diversity. Let  $C(I)$  be the set of unique object categories present in image  $I$ . We discard image  $I$  if:

$$|C(I)| < 3 \quad (2)$$

This guarantees that each selected image contains at least three distinct object categories.

An image  $I$  passes the Vision Content Filter if and only if the following two conditions are satisfied:

$$\forall c \in C(I), \quad N_c(I) \leq 2 \wedge |C(I)| \geq 3 \quad (3)$$

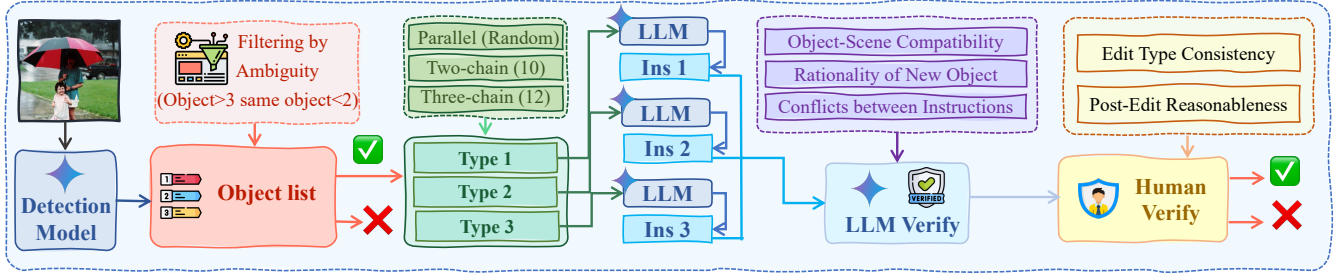


Figure 2: Overview of the data creation pipeline of ComplexBench-Edit.

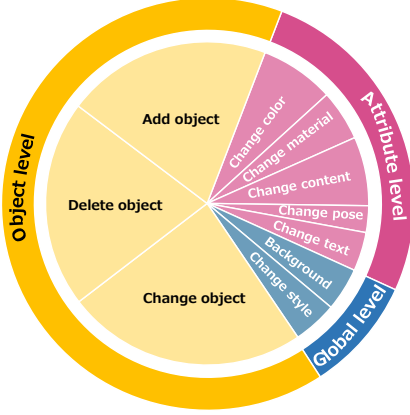


Figure 3: Overview of the three hierarchical levels of editing types in ComplexBench-Edit.

**3.1.2 Type-guided Instruction Generation.** After filtering source images based on visual content, the subsequent step involves generating complex editing instructions. This stage translates curated image data and predefined editing objectives into concrete, executable textual commands for image manipulation. The core mechanism is a MLLM, which takes as input the selected image  $I$ , its object list  $\text{obj}(I)$ , and a chosen combination of editing types. Here,  $\text{obj}(I)$  denotes the list of objects detected in image  $I$ , extracted by a prior object detection module. The MLLM analyzes the image and object-level information in conjunction with the specified editing types, determines appropriate target objects for each operation, and produces precise textual instructions. The structure and complexity of these instructions are governed by predefined editing type combinations, categorized into three hierarchical levels, as shown in Figure 3.

① **Level 1: Parallel.** This level consists of three editing instructions that are logically independent. The order of execution does not affect the final outcome. All three instruction types are randomly sampled from a general set of 10 predefined editing operations.

② **Level 2: Two-chain.** This level includes a two-step dependency chain and one additional independent instruction. Let the instruction types be denoted as  $T_1, T_2, T_3$ , where  $T_1 \rightarrow T_2$  forms a logical dependency and  $T_3$  is independent:

$$\text{Dependent chain: } T_1 \rightarrow T_2 \quad (4)$$

$$\text{Independent instruction: } T_3 \quad (5)$$

Types  $T_1$  and  $T_2$  are sampled from a curated subset of 10 editing types to ensure logical consistency and feasibility (e.g., avoiding

cases where an object is modified after being deleted). The independent type  $T_3$  is sampled from the general editing type set.

③ **Level 3: Three-chain.** This level involves a sequence of three interdependent instructions, forming a three-step chain:

$$T_1 \rightarrow T_2 \rightarrow T_3 \quad (6)$$

All types in this level are sampled from a dedicated subset of 12 editing operations designed to support deeper, logically coherent dependencies.

For levels involving dependent instructions (Two-chain and Three-chain), generation is performed sequentially. When producing an instruction that depends on a previous one, the MLLM receives the previously generated instruction text as additional context:

$$\text{Input}_i = \{I, \text{obj}(I), T_i, T_{i-1}\} \quad (7)$$

This context-aware generation process ensures logical consistency and coherence across dependent editing operations.

**3.1.3 Editing Instruction Feasibility Check.** Following the generation of editing instructions by the MLLM, a crucial step is to validate their feasibility. The complexity of multi-step operations and potential semantic inconsistencies require a rigorous check. We employ a separate validating MLLM that analyzes the generated instructions alongside the source image and object information. A sample (image + instructions) is deemed valid only if it passes checks based on the following criteria:

**1. Object-Scene Compatibility.** Ensures that objects targeted for placement, addition, or movement are semantically consistent and visually plausible within the image’s scene context (e.g., adding a fish to water is compatible; adding it to the sky is not). This prevents instructions that result in unrealistic or nonsensical scenarios.

**2. Rationality of Object Reference and Attributes.** Verifies that references to existing objects are unambiguous. For added or modified objects, it checks if the specified object type and attributes are rational and non-contradictory (e.g., a ‘flying car’ might be rational in some contexts, but ‘invisible, heavy box’ might not be).

**3. Conflicts between Instructions.** For samples with multiple instructions, this criterion identifies potential logical conflicts. It checks if instructions contradict each other or if a step renders a subsequent dependent instruction infeasible (e.g., deleting an object required for a later modification).

Samples that fail any of these feasibility checks are discarded. This validation ensures that the ComplexBench-Edit dataset contains high-quality, executable instructions suitable for benchmarking complex image editing capabilities.

**3.1.4 Human Review.** Despite the MLLM-based feasibility check, a crucial human review stage is performed for benchmark quality assurance. Two PhD students reviewed a subset of generated samples (image + instructions) based on two dimensions:

**1. Edit Type Consistency.** Ensures the generated instruction text accurately reflects the intended editing operation type and category (e.g., Parallel, Two-chain, specific action). This aligns the instruction with the predefined task structure.

**2. Post-Edit Reasonableness.** Evaluates the semantic and visual plausibility of the scene after hypothetically executing the instruction(s). Checks if implied changes or additions are reasonable and coherent within the original image’s context, assessing the logical soundness of the envisioned modified scene.

## 3.2 Automated Evaluation Metrics

To quantitatively evaluate image editing models on ComplexBench-Edit, we define a set of automated evaluation metrics. These metrics assess both the model’s ability to correctly execute complex, multi-step editing instructions and the visual quality and consistency of the generated results.

**3.2.1 Editing Performance Evaluation.** Editing performance is quantitatively evaluated based on the model’s ability to accurately execute both single and chain-dependent instructions. This assessment is performed automatically by a dedicated MLLM evaluator. For each instruction instance, a score is assigned on a 5-point scale (0-5), reflecting the quality of the generated image corresponding to that specific edit. A score of 5 indicates perfect execution, while 0 indicates complete failure or no perceivable attempt. The MLLM evaluator assigns this score by evaluating the edited image against a predefined set of type-specific criteria.

**1. Single-Instruction Evaluation** For independent instructions, the MLLM evaluator assigns a single 5-point score based on the defined criteria for its specific editing type.

**2. Chain-Instruction Evaluation** For instructions forming a dependent chain, the evaluation methodology accounts for the prerequisite nature of earlier steps for the successful execution of subsequent ones. The MLLM evaluator assigns a 5-point score ( $S_i$ ) to each individual instruction  $i$  within the chain, based on its type-specific criteria. The overall performance score for a chain of  $N$  instructions is calculated as the product of the scores of its constituent instructions:

$$S_{chain} = S_1 \times S_2 \times \dots \times S_N \quad (8)$$

This multiplicative approach ensures that failure in any single step (resulting in  $S_i = 0$ ) propagates to the entire chain, yielding a total score of 0 and accurately reflecting the inability to complete the dependent task sequence successfully.

**3.2.2 Vision Consistency Evaluation.** Beyond assessing the performance of the targeted editing operations, it is equally important to evaluate the model’s ability to preserve the original content and visual consistency in the regions of the image that were not intended for modification. Standard pixel-wise metrics like L1 or L2 distance computed over the entire image are inadequate for this purpose, as they would erroneously assign the best scores to models that return the original, unedited image (resulting in a distance of zero), failing to reflect any editing capability.

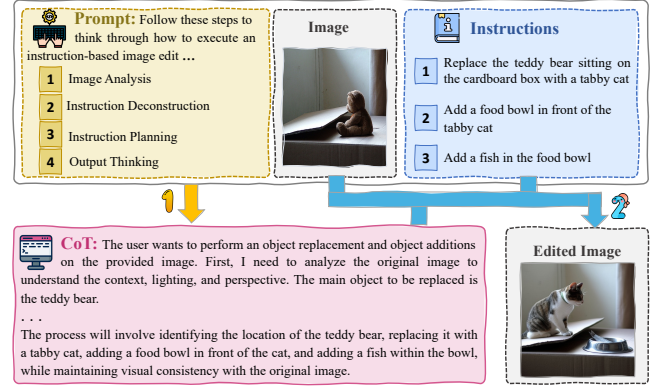


**Figure 4: Diagram of the proposed Chain-of-Thought (CoT) reasoning approach for image editing.**

To address this, we propose a region-specific consistency evaluation. We identify the regions potentially affected by the editing process and exclude them from the consistency calculation. Specifically, we leverage the bounding boxes associated with objects. We consider the ground truth bounding boxes from the original image (available from MSCOCO annotations) and the bounding boxes detected in the edited image using a robust object detection model. Let  $B_{orig}$  be the set of ground truth bounding boxes in the image  $I_{orig}$ , and  $B_{edit}$  be the set of bounding boxes detected in the edited image  $I_{edit}$ . We define the set of regions potentially subject to modification as the union of the areas covered by bounding boxes:

$$R_{edit} = \bigcup_{b \in B_{orig} \cup B_{edit}} \text{Area}(b) \quad (9)$$

where  $\text{Area}(b)$  denotes the region covered by bounding box  $b$ .

The vision consistency is then evaluated on the complementary region,  $R_{consistent} = \text{Image Area} \setminus R_{edit}$ , which represents the parts of the image that should ideally remain unchanged. We compute the consistency using standard pixel-wise distance metrics, specifically the L1 distance and L2 distance, applied only to the pixels within the region  $R_{consistent}$ :

$$L1 = \frac{1}{|R_{consistent}|} \sum_{p \in R_{consistent}} |I_{orig}(p) - I_{edit}(p)| \quad (10)$$

$$L2 = \frac{1}{|R_{consistent}|} \sum_{p \in R_{consistent}} (I_{orig}(p) - I_{edit}(p))^2 \quad (11)$$

where  $|R_{consistent}|$  is the number of pixels in the region  $R_{consistent}$ , and  $I(p)$  denotes the pixel value at location  $p$ . This approach ensures that our consistency metric specifically measures the preservation of the background and non-target content, penalizing unintended modifications or artifacts outside the designated editing areas, without unfairly rewarding models that perform no edits.

## 3.3 CoT Reasoning for Image Editing

In addition to introducing a new benchmark and automated evaluation metrics, we propose a powerful training-free baseline leveraging Chain-of-Thought (CoT) reasoning. Inspired by recent work [13, 21, 30] showing that MLLM-generated CoT enhances instruction understanding in image generation, we apply this to image editing.

**Table 2: Performance comparison on ComplexBench-Edit across different instruction complexity levels: Parallel (Obj., Obj.-At., Obj.-At.-G.), Two-chain (Obj.-At.), and Three-chain (Obj.-At.). “Obj.” denotes Object, “At.” denotes Attribute, and “G.” denotes Global.**

Model	Parallel			Two-chain	Three-chain	Avg.
	Obj.	Obj.-At.	Obj.-At.-G.	Obj.-At.	Obj.-At.	
InstructPix2Pix [5]	9.95	10.45	13.47	4.83	0.52	7.85
MagicBrush [36]	18.29	14.65	11.90	9.70	0.57	11.02
UltraEdit [38]	24.46	25.78	23.80	13.74	3.10	18.18
AnyEdit [34]	13.51	11.27	9.33	6.61	1.01	8.35
VAR-GPT [41]	0.86	0.39	3.80	0.54	0.00	1.12
SEED-LLAMA [12]	5.59	5.93	6.00	4.48	0.27	4.46
OmniGen [31]	32.34	26.57	30.90	16.96	4.36	22.23
GoT [9]	20.09	14.85	16.42	11.76	0.93	12.81
ICEdit [37]	32.97	26.96	27.07	21.80	8.09	23.38
Step1X-Edit [19]	32.61	30.14	31.57	19.56	6.34	24.05
Gemini [28]	49.31	43.47	37.23	38.35	15.10	36.70
Ours (Gemini-CoT)	51.76	50.11	43.08	39.85	17.54	40.47

As shown in Figure 4, our baseline employs a separate MLLM to generate a detailed CoT rationale for executing a given instruction on the source image. A specific prompt is used to guide the MLLM’s thought process, encouraging it to: 1) Analyze the image context, 2) Deconstruct the user instruction into specific operations, 3) Plan the spatial and sequential execution of these operations, and 4) Construct a conceptual output or execution blueprint.

The generated CoT is then concatenated with the original user instruction. This combined input string is provided to the image editing model. This approach aims to provide the editing model with a richer, reasoned understanding of the task, facilitating improved performance without requiring task-specific fine-tuning.

## 4 Experiments

### 4.1 Comparison Methods

We evaluate the performance on ComplexBench-Edit against a comprehensive suite of recent image editing models. These include established instruction-based methods like InstructPix2Pix [5], MagicBrush [36], UltraEdit [38], ICEdit [37], and AnyEdit [34]. We also benchmark against models that integrate LLMs for improved instruction comprehension and editing, such as SEED-LLAMA [12], OmniGen [31], and Step1X-Edit [19]. Additionally, we include VAR-GPT [41] and GoT [9]. Finally, we use the powerful proprietary MLLM, Gemini [28], as a strong baseline editor, and compare it with our proposed Gemini-CoT method, which augments Gemini with Chain-of-Thought reasoning.

### 4.2 Editing Performance Evaluation

**Evaluation with Different Complex-levels** Table 2 shows performance across varying instruction complexities. Our **Gemini-CoT** method consistently achieves the highest scores, excelling at Parallel, Two-chain, and Three-chain instructions, with CoT reasoning providing a clear advantage over the strong standard Gemini. Performance generally degrades with increased complexity, as most models struggle significantly with chained dependencies. While recent models like Step1X-Edit and ICEdit show improvements, they lag behind Gemini-based approaches, especially in longer dependency chains where Gemini-CoT leads substantially. It shows challenge of sequential edits and efficacy of our method.

**CoT:** The user wants to modify the original image by adding two new objects and changing the color of one of them. First, I need to analyze the original image to understand the scene (a white plate with orange peels). Then, I will deconstruct the user’s instructions into three distinct operations: adding a whole orange, adding an orange slice, and recoloring the orange slice. I will plan the placement of the new objects based on the specified locations ('top left of the plate' and 'below the whole orange'). Finally, I will describe the visual modifications, ensuring the recoloring applies only to the newly added orange slice and the existing elements remain unchanged..

#### Multi Instruction:

1. Add whole orange at the top left of the plate
2. Add orange slice below the whole orange
3. Change the color of orange slice to green



↓ Gemini

w/ CoT



w/o CoT



**Figure 5: Comparison of image editing results w/ and w/o CoT.**

**Evaluation with Different Complex-types** Table 3 details performance across 10 distinct editing types. **Gemini-CoT** again shows broad superiority, leading across most object, attribute, and global-level edits. Vanilla Gemini also excels, with CoT notably boosting performance, particularly for complex object and attribute modifications. While some models show niche strengths (e.g., Step1X-Edit in “Change Style”), many struggle with types like “Change Pose” or “Change Text” compared to Gemini variants. Results highlight MLLM approaches like Gemini and our Gemini-CoT set benchmark.

### 4.3 Vision Consistency Evaluation

Table 4 presents the vision consistency results, measured by L1 and L2 distances (lower is better) in non-edited regions across various instruction complexities. **OmniGen** [31] exhibits superior consistency, achieving the best average L1 (0.0377) and L2 (0.0068) scores. It consistently minimizes alterations in unchanged areas across all tested scenarios. Other models like **ICEdit** [37], **Step1X-Edit** [19], and **UltraEdit** [38] also demonstrate strong preservation capabilities. UltraEdit is particularly effective in L2 distance, ranking second on average. Conversely, **Gemini** [28] and **Ours (Gemini-CoT)**, despite their leading editing performance, show higher L1/L2 scores here, suggesting their extensive edits might impact surrounding regions more. Models like SEED-LLAMA show the least consistency, with significantly higher error scores. This indicates a potential trade-off between aggressive editing and background preservation, where OmniGen currently offers the best balance.

### 4.4 Effect of Vision CoT

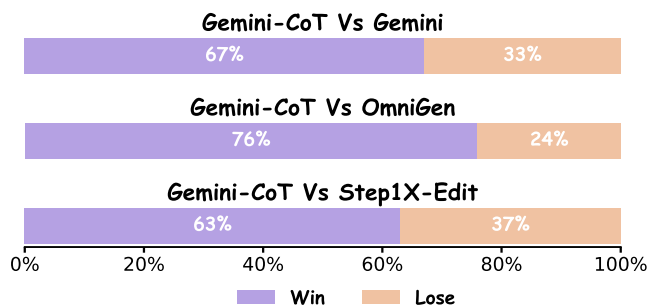
Figure 5 illustrates CoT reasoning’s benefit for complex image editing, exemplified by a multi-step instruction to add and modify

**Table 3: Performance comparison of models across 10 distinct editing types, categorized into Object-level, Attribute-level, and Global-level.**

Model	Object-level			Attribute-level					Global-level	
	Add Object	Change Object	Delete Object	Change Color	Change Pose	Change Material	Change Content	Change Text	Change Background	Change Style
InstructPix2Pix [5]	11.10	10.51	12.50	13.98	9.09	9.38	12.82	2.11	9.70	18.02
MagicBrush [36]	13.96	14.06	22.97	11.84	9.55	9.07	13.94	7.11	10.91	4.36
UltraEdit [38]	24.63	24.12	29.59	24.20	9.52	17.11	29.22	17.63	19.59	25.35
AnyEdit [34]	9.90	8.83	16.83	20.00	5.91	5.57	13.66	8.42	6.67	0.99
VAR-GPT [41]	1.77	0.51	4.27	0.00	1.82	0.41	0.56	0.00	0.40	3.37
SEED-LLAMA [12]	5.31	5.48	8.82	2.91	8.16	5.57	3.10	0.79	5.66	6.34
OmniGen [31]	22.83	26.29	42.45	27.77	8.18	15.00	33.66	16.84	17.17	<u>44.75</u>
GoT [9]	15.18	15.18	26.73	9.32	6.82	11.13	11.69	2.89	11.52	25.80
ICEdit [37]	30.31	31.22	26.52	<u>41.55</u>	7.73	16.08	34.93	17.37	17.38	42.18
Step1X-Edit [19]	32.29	30.91	33.48	34.56	10.00	<u>22.06</u>	38.45	25.26	16.97	<b>45.54</b>
Gemini [28]	47.87	42.63	56.99	36.38	<b>52.38</b>	19.78	<b>46.07</b>	26.93	31.22	16.97
Ours (Gemini-CoT)	<b>48.23</b>	<b>44.78</b>	<b>66.38</b>	<b>41.98</b>	<u>51.36</u>	<b>32.50</b>	<u>45.82</u>	<b>28.68</b>	<b>38.98</b>	30.69

**Table 4: Vision consistency evaluation (L1 and L2 distances, lower is better) on non-edited regions across instruction complexities.**

Model	Parallel				Two-chain		Three-chain		Avg.	
	Object		Object-attribute		Object-attribute		Object-attribute		L1 ↓	L2 ↓
	L1 ↓	L2 ↓	L1 ↓	L2 ↓	L1 ↓	L2 ↓	L1 ↓	L2 ↓	L1 ↓	L2 ↓
InstructPix2Pix [5]	0.1663	0.0588	0.1581	0.0560	0.1696	0.0617	0.1374	0.0428	0.1578	0.0548
MagicBrush [36]	0.0701	0.0233	0.0707	0.0242	0.0609	0.0210	0.0599	0.0180	0.0654	0.0216
UltraEdit [38]	0.0568	0.0098	0.0522	<u>0.0081</u>	0.0556	<u>0.0092</u>	0.0596	0.0099	0.0560	<u>0.0092</u>
AnyEdit [34]	0.0685	0.0239	0.0602	0.0194	0.0747	0.0292	0.0424	<u>0.0078</u>	0.0614	0.0201
VAR-GPT [41]	0.2539	0.1165	0.2421	0.1112	0.2400	0.1066	0.2390	0.1038	0.2437	0.1095
SEED-LLAMA [12]	0.2763	0.1223	0.2754	0.1213	0.2716	0.1184	0.2727	0.1174	0.2740	0.1198
OmniGen [31]	<b>0.0392</b>	<b>0.0071</b>	<b>0.0352</b>	<b>0.0059</b>	<b>0.0381</b>	<b>0.0079</b>	<b>0.0382</b>	<b>0.0062</b>	<b>0.0377</b>	<b>0.0068</b>
GoT [9]	0.0730	0.0287	0.0819	0.0351	0.0564	0.0221	0.0587	0.0219	0.0675	0.0269
ICEdit [37]	<u>0.0422</u>	<u>0.0095</u>	0.0411	0.0104	0.0471	0.0131	<u>0.0397</u>	0.0083	<u>0.0425</u>	0.0103
Step1X-Edit [19]	0.0462	0.0157	<u>0.0392</u>	0.0113	<u>0.0413</u>	0.0130	0.0498	0.0155	0.0441	0.0139
Gemini [28]	0.0657	0.0192	0.0559	0.0159	0.0634	0.0197	0.0531	0.0129	0.0595	0.0169
Ours (Gemini-CoT)	0.0982	0.0348	0.0718	0.0209	0.0823	0.0292	0.0863	0.0273	0.0846	0.0281

**Figure 6: Human evaluation between Gemini-CoT and others.**

oranges. CoT provides a structured thought process (analyzing, deconstructing, planning). With CoT guidance, the Gemini model more accurately executes instructions, adding the whole orange and a green fruit element as intended. Without CoT, it struggles, producing a less faithful result that fails to correctly add a distinct slice or apply the color change. This comparison highlights how CoT enhances the model’s ability to understand and execute complex, sequential edits, improving alignment with user intent.

## 4.5 Human Evaluation

To complement automated metrics, we conducted human evaluations assessing the perceptual quality of edits from our Gemini-CoT method against leading models. As shown in Figure 6, evaluators performed pairwise comparisons. Results indicate a strong preference for Gemini-CoT: it was preferred over standard Gemini in 67% of cases, over OmniGen in 76%, and over Step1X-Edit in 63%. These findings highlight CoT’s effectiveness in producing edits that are quantitatively superior and better aligned with human perception of quality and instruction adherence.

## 5 Conclusion

We introduced ComplexBench-Edit, a novel benchmark for evaluating image editing models on complex, multi-instruction tasks, especially chained dependencies. We also presented Gemini-CoT, a training-free method using Chain-of-Thought reasoning, which significantly enhanced the execution of these intricate instructions. Experiments demonstrated Gemini-CoT’s superior performance where many existing models struggle, particularly with sequential edits, a finding corroborated by human evaluations.

## References

- [1] Marah Abdin, Jyoti Aneja, Hany Awadalla, Ahmed Awadallah, Ammar Ahmad Awan, Nguyen Bach, Amit Bahree, Arash Bakhtiari, Jianmin Bao, Harkirat Behl, et al. 2024. Phi-3 technical report: A highly capable language model locally on your phone. *arXiv preprint arXiv:2404.14219* (2024).
- [2] Jacob Austin, Daniel D. Johnson, Jonathan Ho, Daniel Tarlow, and Rianne van den Berg. 2021. Structured Denoising Diffusion Models in Discrete State-Spaces. In *NeurIPS*.
- [3] Jinbin Bai, Wei Chow, Ling Yang, Xiangtai Li, Juncheng Li, Hanwang Zhang, and Shuicheng Yan. 2024. HumanEdit: A High-Quality Human-Rewarded Dataset for Instruction-based Image Editing. *arXiv preprint arXiv:2412.04280* (2024).
- [4] Shuai Bai, Keqin Chen, Xuejing Liu, Jialin Wang, Wenbin Ge, Sibao Song, Kai Dang, Peng Wang, Shijie Wang, Jun Tang, et al. 2025. Qwen2. 5-vl technical report. *arXiv preprint arXiv:2502.13923* (2025).
- [5] Tim Brooks, Aleksander Holynski, and Alexei A Efros. 2023. Instructpix2pix: Learning to follow image editing instructions. In *Proceedings of the IEEE/CVF conference on computer vision and pattern recognition*. 18392–18402.
- [6] Tom Brown, Benjamin Mann, Nick Ryder, Melanie Subbiah, Jared D Kaplan, Prafulla Dhariwal, Arvind Neelakantan, Pranav Shyam, Girish Sastry, Amanda Askell, et al. 2020. Language models are few-shot learners. *Advances in neural information processing systems* 33 (2020), 1877–1901.
- [7] Goirik Chakrabarty, Aditya Chandrasekar, Ramya Hebbalaguppe, and Prathosh AP. 2024. Lomoe: Localized multi-object editing via multi-diffusion. In *Proceedings of the 32nd ACM International Conference on Multimedia*. 3342–3351.
- [8] Patrick Esser, Sumith Kulal, Andreas Blattmann, Rahim Entezari, Jonas Müller, Harry Saini, Yam Levi, Dominik Lorenz, Axel Sauer, Frederic Boesel, et al. 2024. Scaling rectified flow transformers for high-resolution image synthesis. In *Forty-first international conference on machine learning*.
- [9] Rongyao Fang, Chengqi Duan, Kun Wang, Linjiang Huang, Hao Li, Shilin Yan, Hao Tian, Xingyu Zeng, Rui Zhao, Jifeng Dai, et al. 2025. Got: Unleashing reasoning capability of multimodal large language model for visual generation and editing. *arXiv preprint arXiv:2503.10639* (2025).
- [10] Tsu-Jui Fu, Wenze Hu, Xianzhi Du, William Yang Wang, Yinfei Yang, and Zhe Gan. 2024. Guiding Instruction-based Image Editing via Multimodal Large Language Models. In *ICLR*.
- [11] Yuying Ge, Sijie Zhao, Chen Li, Yixiao Ge, and Ying Shan. 2024. Seed-data-edit technical report: A hybrid dataset for instructional image editing. *arXiv preprint arXiv:2405.04007* (2024).
- [12] Yuying Ge, Sijie Zhao, Ziyun Zeng, Yixiao Ge, Chen Li, Xintao Wang, and Ying Shan. 2024. Making LLaMA SEE and Draw with SEED Tokenizer. In *ICLR 2024*.
- [13] Ziyu Guo, Renrui Zhang, Chengzhuo Tong, Zhizheng Zhao, Peng Gao, Hongsheng Li, and Pheng-Ann Heng. 2025. Can We Generate Images with CoT? Let's Verify and Reinforce Image Generation Step by Step. *arXiv preprint arXiv:2501.13926* (2025).
- [14] Amir Hertz, Ron Mokady, Jay Tenenbaum, Kfir Aberman, Yael Pritch, and Daniel Cohen-Or. 2022. Prompt-to-prompt image editing with cross attention control. *arXiv preprint arXiv:2208.01626* (2022).
- [15] Jonathan Ho, Ajay Jain, and Pieter Abbeel. 2020. Denoising Diffusion Probabilistic Models. In *NeurIPS 2020*.
- [16] Mingzhen Huang, Jialing Cai, Shan Jia, Vishnu Lokhande, and Siwei Lyu. 2024. ParallelEdits: Efficient Multi-Aspect Text-Driven Image Editing with Attention Grouping. *Advances in Neural Information Processing Systems* 37 (2024), 22569–22595.
- [17] Yuzhou Huang, Liangbin Xie, Xintao Wang, Ziyang Yuan, Xiaodong Cun, Yixiao Ge, Jiantao Zhou, Chao Dong, Rui Huang, Ruimao Zhang, et al. 2024. Smartedit: Exploring complex instruction-based image editing with multimodal large language models. In *Proceedings of the IEEE/CVF Conference on Computer Vision and Pattern Recognition*. 8362–8371.
- [18] Tsung-Yi Lin, Michael Maire, Serge Belongie, James Hays, Pietro Perona, Deva Ramanan, Piotr Dollár, and C Lawrence Zitnick. 2014. Microsoft coco: Common objects in context. In *ECCV*. 740–755.
- [19] Shiyu Liu, Yucheng Han, Peng Xing, Fukun Yin, Rui Wang, Wei Cheng, Jiaqi Liao, Yingming Wang, Honghao Fu, Chunrui Han, et al. 2025. Step1X-Edit: A Practical Framework for General Image Editing. *arXiv preprint arXiv:2504.17761* (2025).
- [20] Yiwei Ma, Jiayi Ji, Ke Ye, Weihuang Lin, Zhibin Wang, Yonghan Zheng, Qiang Zhou, Xiaoshuai Sun, and Rongrong Ji. 2024. I2EBench: A Comprehensive Benchmark for Instruction-based Image Editing. In *NeurIPS*.
- [21] Chancharik Mitra, Brandon Huang, Trevor Darrell, and Roei Herzig. 2024. Compositional chain-of-thought prompting for large multimodal models. In *Proceedings of the IEEE/CVF Conference on Computer Vision and Pattern Recognition*. 14420–14431.
- [22] William Peebles and Saining Xie. 2023. Scalable diffusion models with transformers. In *Proceedings of the IEEE/CVF international conference on computer vision*. 4195–4205.
- [23] Dustin Podell, Zion English, Kyle Lacey, Andreas Blattmann, Tim Dockhorn, Jonas Müller, Joe Penna, and Robin Rombach. 2023. Sdxl: Improving latent diffusion models for high-resolution image synthesis. *arXiv preprint arXiv:2307.01952* (2023).
- [24] Alec Radford, Jong Wook Kim, Chris Hallacy, Aditya Ramesh, Gabriel Goh, Sandhini Agarwal, Girish Sastry, Amanda Askell, Pamela Mishkin, Jack Clark, et al. 2021. Learning transferable visual models from natural language supervision. In *International conference on machine learning*. PmlR, 8748–8763.
- [25] Robin Rombach, Andreas Blattmann, Dominik Lorenz, Patrick Esser, and Björn Ommer. 2022. High-resolution image synthesis with latent diffusion models. In *Proceedings of the IEEE/CVF conference on computer vision and pattern recognition*. 10684–10695.
- [26] Shelly Sheynin, Adam Polyak, Uriel Singer, Yuval Kirstain, Amit Zohar, Oron Ashual, Devi Parikh, and Yaniv Taigman. 2024. Emu edit: Precise image editing via recognition and generation tasks. In *Proceedings of the IEEE/CVF Conference on Computer Vision and Pattern Recognition*. 8871–8879.
- [27] Yang Song, Jascha Sohl-Dickstein, Diederik P Kingma, Abhishek Kumar, Stefano Ermon, and Ben Poole. 2020. Score-based generative modeling through stochastic differential equations. *arXiv preprint arXiv:2011.13456* (2020).
- [28] Gemini Team, Rohan Anil, Sebastian Borgeaud, Jean-Baptiste Alayrac, Jiahui Yu, Radu Soricut, Johan Schalkwyk, Andrew M Dai, Anja Hauth, Katie Millican, et al. 2023. Gemini: a family of highly capable multimodal models. *arXiv preprint arXiv:2312.11805* (2023).
- [29] Chenglin Wang, Yucheng Zhou, Zijie Zhai, Jianbing Shen, and Kai Zhang. 2024. Diffusion model with representation alignment for protein inverse folding. *arXiv preprint arXiv:2412.09380* (2024).
- [30] Jason Wei, Xuezhi Wang, Dale Schuurmans, Maarten Bosma, Fei Xia, Ed Chi, Quoc V Le, Denny Zhou, et al. 2022. Chain-of-thought prompting elicits reasoning in large language models. *Advances in neural information processing systems* 35 (2022), 24824–24837.
- [31] Shitao Xiao, Yuezhe Wang, Junjie Zhou, Huaying Yuan, Xingrun Xing, Ruiran Yan, Chaofan Li, Shuting Wang, Tiejun Huang, and Zheng Liu. 2024. Omnigen: Unified image generation. *arXiv preprint arXiv:2409.11340* (2024).
- [32] Siwei Yang, Mude Hui, Bingchen Zhao, Yuyin Zhou, Nataniel Ruiz, and Cihang Xie. 2025. Complex-Edit: CoT-Like Instruction Generation for Complexity-Controllable Image Editing Benchmark. *arXiv preprint arXiv:2504.13143* (2025).
- [33] Zhen Yang, Ganggui Ding, Wen Wang, Hao Chen, Bohan Zhuang, and Chunhua Shen. 2023. Object-aware inversion and reassembly for image editing. *arXiv preprint arXiv:2310.12149* (2023).
- [34] Qifan Yu, Wei Chow, Zhongqi Yue, Kaihang Pan, Yang Wu, Xiaoyang Wan, Juncheng Li, Siliang Tang, Hanwang Zhang, and Yueting Zhuang. 2024. AnyEdit: Mastering Unified High-Quality Image Editing for Any Idea. *arXiv preprint arXiv:2411.15738* (2024).
- [35] Hao Zhang, Feng Li, Shilong Liu, Lei Zhang, Hang Su, Jun Zhu, Lionel M Ni, and Heung-Yeung Shum. 2022. Dino: Detr with improved denoising anchor boxes for end-to-end object detection. *arXiv preprint arXiv:2203.03605* (2022).
- [36] Kai Zhang, Lingbo Mo, Wenhui Chen, Huan Sun, and Yu Su. 2023. Magicbrush: A manually annotated dataset for instruction-guided image editing. *Advances in Neural Information Processing Systems* 36 (2023), 31428–31449.
- [37] Zechuan Zhang, Ji Xie, Yu Lu, Zongxin Yang, and Yi Yang. 2025. In-Context Edit: Enabling Instructional Image Editing with In-Context Generation in Large Scale Diffusion Transformer. *arXiv preprint arXiv:2504.20690* (2025).
- [38] Haozhe Zhao, Xiaojian Shawn Ma, Liang Chen, Shuzheng Si, Rujie Wu, Kaikai An, Peiyu Yu, Minjia Zhang, Qing Li, and Baobao Chang. 2024. Ultraedit: Instruction-based fine-grained image editing at scale. *Advances in Neural Information Processing Systems* 37 (2024), 3058–3093.
- [39] Yucheng Zhou, Xiang Li, Qianning Wang, and Jianbing Shen. 2024. Visual in-context learning for large vision-language models. *arXiv preprint arXiv:2402.11574* (2024).
- [40] Yucheng Zhou, Jianbing Shen, and Yu Cheng. 2025. Weak to strong generalization for large language models with multi-capabilities. In *The Thirteenth International Conference on Learning Representations*.
- [41] Xianwei Zhuang, Yuxin Xie, Yufan Deng, Liming Liang, Jinghan Ru, Yuguo Yin, and Yuexian Zou. 2025. VARGPT: Unified Understanding and Generation in a Visual Autoregressive Multimodal Large Language Model. *arXiv preprint arXiv:2501.12327* (2025).